Moment-to-moment fluctuations of hemodynamic responses in posterior default mode networks differentially predict level of attentional lapses in adolescents with Attention-Deficit/Hyperactivity Disorder

Lin Sørensen[1], Yu Sun Chung[2], Sabin Khadka[2] & Michael C. Stevens[2,3]

[1]Department of Biological and Medical Psychology, University of Bergen, Bergen, Norway

[2]Olin Neuropsychiatry Research Center, Institute of Living, Hartford, CT, United States

[3]Department of Psychiatry, Yale University School of Medicine, New Haven, CT, United States

Correspondence:

Lin Sørensen

Department of Biological and Medical Psychology

University of Bergen

Jonas Liesvei 91

5009 Bergen

E-mail: Lin.Sorensen@uib.no

Abstract

Background: The neurobiological underpinnings of the characteristically higher intra-individual variability of reaction times (IIVRT) in patients with ADHD remain poorly understood. The aim of the current study was to characterize the role of the default mode and other canonical brain networks measured by functional magnetic resonance imaging (fMRI) to the moment-to-moment task performance fluctuations measured by IIVRT. To our knowledge, no prior fMRI study has shown the involvement of posterior default mode network (DMN) in ADHD IIVRT. We expected that moment-to-moment fluctuations in hemodynamic responses in posterior DMN would predict higher IIVRT specifically in ADHD.

Methods: Adolescents (12 to 19 years old) with ADHD (n= 55) and healthy controls (n= 55) performed a fMRI Go/NoGo task. Whole-brain independent component analysis (ICA) segregated hemodynamic responses into functional brain networks, then further decomposed into individual trial-specific estimates of hemodynamic response amplitude. Mean and variability metrics of these amplitudes were tested in stepwise linear regression analyses to identify which functional brain networks predicted high IIVRT.

Results: As expected, variability in hemodynamic responses in posterior DMN regions predicted level of IIVRT. In posterior cingulate cortex this variability predicted higher IIVRT only in ADHD, whereas in precuneus variability in hemodynamic responses predicted lower IIVRT. Average hemodynamic responses in a bilateral superior temporal cortex network predicted higher IIVRT only in ADHD.

Conclusion: Our findings suggest that estimating variability in hemodynamic responses is crucial to understand the involvement of the intrinsic default mode in attentional lapses in ADHD. The parcellation into posterior default mode subnetworks showed the differentiating role of default mode in attentional lapses in ADHD.

Attention-Deficit/Hyperactivity Disorder (ADHD) is a highly prevalent neurodevelopment disorder observed in about 5% of children and adolescents (1). It is a behaviorally defined disorder with age-inappropriate, elevated symptoms of inattention. One of the most consistently found abnormalities in ADHD found on cognitive tests is that lapses in attention occur more frequently than in healthy controls (2-5) (hedges' *g* effect size = 0.76, or "large") (3). In research studies, attentional lapses are typically operationalized as moment-to-moment fluctuations in task-performance measured with intra-individual reaction time variability (IIVRT), and sometimes as longer mean reaction times (RTs) (2, 4-6). IIVRT can occur in many different cognitive contexts (7) (e.g., in paradigms that measure attention or cognitive control (5)), but appears to be unique from other shared performance characteristics like response speed (3, 8). IIVRT is a candidate endophenotype for ADHD. It not only has a genetic basis (9, 10) and appears to be a lifetime trait (REF), IIVRT predicts academic performance in children with ADHD (11), can differentiate ADHD from autism(8, 12), and there is evidence suggesting IIVRT abnormalities are attenuated by psychostimulant ADHD medications (3). Despite these numerous indicators that IIVRT is an important ADHD biomarker, its exact neurobiological underpinnings are still poorly understood.

One dominant hypothesis that has been tested extensively is that attentional lapses stem from spontaneous activity within the brain's intrinsic default mode network (DMN) that interrupts goal-directed "task-positive" brain activation (6, 13, 14). The DMN is a collection of core functional hubs (medial prefrontal cortex (mPFC), posterior cingulate cortex (PCC) and precuneus) with high baseline levels of activity that seem to shift back-and-forth from a "default" state to an active cognitively demanding state (13). Performing externally-oriented, demanding attention tasks will normally lead to suppression of the DMN spontaneous activity (6, 13, 14). In ADHD, it has been hypothesized that spontaneous activity within the DMN persists and might

interrupt attention processing, causing fluctuations in reaction times and high IIVRT (15, 16). In resting-state fMRI studies, DMN activation has been shown to be abnormally higher in ADHD (17 – 21), while the typical inverse correlation between DMN activity and task-based cognitive control network hubs appears weaker and to suffer from a maturational lag in ADHD (17-21). ADHD IIVRT is associated with mean hemodynamic responses (HRs) in the anterior DMN regions of mPFC during working memory processing (22) and during attention oddball task processing (23). There also is evidence that links behavioral IIVRT to variability in the hemodynamic response itself within brain regions that comprise the anterior DMN (24). Importantly, this latter study was the first to show IIVRT was not simply the result of weaker or lower brain activity, but more specifically related to the inconsistency of response to attention-eliciting stimuli on an oddball attention task.

Although such studies have greatly advanced our understanding ADHD neural dysfunction underlying IIVRT, the posterior DMN regions have not yet been linked to IIVRT in ADHD. This absence of evidence is meaningful, as in some ways the posterior DMN represents a more likely, logical neurobiological influence over attention fluctuations. Several studies suggest posterior DMN is especially important for the transition between the low-frequency resting-state brain activation and the down-regulation of this fluctuation during task-positive activation of attention networks in the brain (13, 25, 26). Interestingly, in fMRI meta-analyses of Go/NoGo tasks, individuals with ADHD typically show hyperactivation – or what could be interpreted as lower deregulation (27) – of the posterior DMN areas of the precuneus/PCC during motor inhibition (NoGo) (27-29). However, none of these studies have shown an association between DMN regions and ADHD IIVRT. High IIVRT in ADHD instead has been associated with mean hemodynamic responses in frontoparietal attention networks (30, 31) and temporal areas (32). Also, attentional lapses as estimated with the ex-gaussian distribution of reaction

times (tau) on Go trials was not associated with mean amplitude of hemodynamic responses in any functional brain network (33). Because these latter findings do not strictly comport with the DMN interruption hypothesis, they raise the possibility the underlying neural mechanism of IIVRT-related ADHD dysfunction might be different, more complex, or more extensive than is currently thought (16). For instance, high IIVRT in ADHD could stem from abnormal motor response preparations and selection involving the pre-motor systems (34), or even temporal processing deficits involving other cortex (2, 23, 32). There is a need to more rigorously interrogate all possibly-relevant brain systems to aid ADHD IIVRT neurobiological modeling-building efforts.

Accordingly, the goals of this study were a) to concurrently evaluate task-elicited responsiveness and variability within all the brain's major neural systems to determine which are linked to high IIVRT and are dysfunctional in ADHD, while retaining a specific focus on DMN as the leading candidate neural system, and b) to extend prior findings of IIVRT-related neurobiology learned primarily from attention paradigms by examining a moderate-sized adolescent non-ADHD and ADHD sample who performed a Go/NoGo fMRI task (35). We predicted that Go/NoGo task hemodynamic response amplitude variability in both anterior and posterior DMN hub regions would predict higher ADHD IIVRT (24, 36, 37). Secondary expectations included that mean amplitude would predict similarly as previous Go/NoGo fMRI studies higher IIVRT in pre-motor systems (31, 38) and temporal lobe cortex (2, 23).

Methods and Materials

Participants

The sample (N=110) consisted of adolescents with ADHD (n=55) and healthy controls between 12 and 19 years old (M=15.40, SD=1.77). Experienced clinical staff members conducted

a diagnostic evaluation with the Schedule for Affective Disorders and Schizophrenia for School-Age Children-Present and Lifetime Version (K-SADS-PL) (39). In the ADHD group, 49 were diagnosed with the DSM-V Combined-Type ADHD, 1 with predominantly inattentive ADHD and 5 with an ADHD in remission. Comorbid disorders were as typically reported (40) present in the ADHD group: Oppositional Defiant Disorder (*n*=10), Conduct Disorder (*n*=4), Anxiety and Depressive Disorders (*n*=6), and Dependence/Abuse disorders (*n*=7). In the control group, 1 had a depressive disorder and 1 had a Dependence Disorder. Full Scale intelligence (IQ) was estimated based on Matrix Reasoning and Vocabulary subtests of the Wechsler Abbreviated Scale of Intelligence (WASI) (41). ADHD participants who took medication followed a 24-hour washout procedure prior to the cognitive and MRI assessments. All participants and/or their parents gave informed consent following the procedures approved by Hartford Hospital's Institutional Review Board and in accordance with the Helsinki declaration.

fMRI task and procedure: Go/NoGo task

Participants performed two sessions of an event-related fMRI Go/NoGo task consisting of frequent "X" and infrequent "K" stimuli presented for 50 msec each (35, 42). Each lasted 7:21 min and consisted of 246 trials, in which the "K" stimulus was presented in 16% of the trials with intervals in the range of 10-15 seconds. Participants were instructed to make a speeded button press with their right index finger to rapidly presented stimuli of "X" (Go), but to withhold response to pseudo-randomly interspersed "K" (NoGo) stimuli. The participants first performed a practice trial to ensure they understood the instructions. Hits and errors were registered as a response if occurring within 1,000 msec of an "X" or "K" trial, respectively. IIVRT and mean reaction times were estimated by calculating standard deviations and means for each participant across all Go-trials in the two sessions.

The Go/NoGo task was implemented using the E-Prime 2.0 (Psychology Software Tools, Inc.). The experimental stimuli were projected via a screen visible to the participants in the MRI by a rear-facing mirror attached to the head coil. Behavioral responses were registered using a fiber-optic MRI-compatible response device (Current Designs, Inc.) and recorded by E-Prime for off-line analyses.

MRI Scanning Parameters

MR imaging were performed with a 3.0 Tesla Siemens Allegra MRI scanner at the Olin Neuropsychiatric Research Center, Institute of Living at Hartford Hospital. Functional image volumes were collected using gradient-echo echo-planar imaging (EPI) pulse sequence: repetition time (TR)=1500 msec, echo time (TE)=28 msec, flip angle=65°, field of view=24x24 cm, acquisition matrix=64x64, A>>P phase encoding, voxel size=3.4x3.4 mm, slice thickness=5 mm, number of slices=29 (acquired sequentially). Gradient echo fieldmaps: TR=580 msec, TE=7 msec, flip angle=90°, matrix=128x128, A>>P phase encoding, 3 mm slice thickness, MPRAGE T1-weighted images of brain structure: TR=2500 msec, TE=2.74 msec, flip angle=8°, matrix=256x208, 1 mm slice thickness.

Image Processing

Each of the fMRI time series was realigned to the mid-series volume (43), corrected for slice-timing acquisition differences (44). Spatial distortions were removed when due to inhomogeneity according to fieldmap-based unwarping (45). Signal spikes were removed using AFNI 3Despike (46) and volumes were automatically reoriented to sterotactic space using 3-parameter rigid body realignment. Spatial normalization parameters mapping the T1 to MNI atlas space were applied to each fMRI volume. Each image was written at 3 mm^3 isotropic voxel resolution and thereafter spatially smoothed with a 6 mm FWHM Gaussian kernel. Variance in

time series due to had motion was removed and the data linearly detrended using fMRIB's ICA-based Xnoiseifier (FIX v1.602 beta) (47). In addition, the fMRI data were also visually inspected in case of sudden head displacements greater than a voxel length.

Independence component analysis (ICA)

A group-level ICA was performed with subsequent extraction of single-trial estimates and regression as described in Eichele et al. (37). This allowed for analyzing the temporal dynamics of successive task-trials of the Go/NoGo. The ICA functionally segregates individual or small groups of brain regions with unique time courses (48, 49). The preprocessed data were decomposed into 100 components using a high model order ICA with the GIFT toolbox (https://trendscenter.org/software/gift/). Spatial ICA maps were generated with the Infomax algorithm (37, 50). Regression analysis was used to back construct participant-specific time-courses (51). 32 components were selected for analysis, based on whether or not each was task-related, i.e., had hemodynamic timecourses that correlated with a conventional fMRI model of Go/NoGo task onsets for correct rejections, commission errors, and hits across the entire group of participants. For these components, single-trial estimates of means and standard deviations of the hemodynamic responses then were calculated for each participant. The single-trial mean of amplitudes is comparable to simple activation from conventional fMRI time series calculated with GLM analysis. Next, intra-individual standard deviations of single-trial hemodynamic responses across trials were estimated to measure variability in these response amplitudes. Larger standard deviations reflect greater intra-individual trial-to-trial hemodynamic response variability (52).

Testing the prediction of single-trial amplitude ICs on level of IIVRT

All statistical analyses were performed with the IBM SPSS version 26. Between-group analyses were conducted to investigate effects of ADHD on level of IIVRT, and bivariate correlational analyses to study the relationship between the ICs. Prior to modeling, data outliers were defined by calculating the median absolute deviation (MAD), using a threshold of +/- 3 for calculating the deviation distance from the center in terms (53). Across the 32 ICs of hemodynamic response variability and mean measurements over all types of trials (192 variables), 1.7% outlier cases in average were detected. These infrequent outlier cases were replaced with *M* +/- 3**MAD* scores.

To test which functional brain networks would predict level of IIVRT, stepwise (forward) linear regression analyses were conducted. In all models, age, sex, and IQ were included as covariates. All models used IIVRT as the outcome variable and the single-trial mean and variability for each of the 32 ICs and the diagnoses of ADHD as predictors, both as main effects and as interaction effect terms (ICs x ADHD). Three of these models used Correct Reject, False Alarm and Hit hemodynamic response variability for the ICs, while another three used hemodynamic response mean. The stepwise procedure involved conducting multiple linear regression analyses several times, each step removing the variables with weakest correlation with the outcome variable of IIVRT. To maximize predicted variance of each of the models, we focused on the last regression model to reach significance. This last model was bootstrapped as a resampling procedure.

The overall regression models were:

$$IIVRT = b_0 + b_1 Age + b_2 Sex + b_3 IQ + b_4 ADHD + b_k ICs\ of\ amplitude\ variability + b_k ICs\ of\ amplitude\ variability\ x\ ADHD$$

The significance threshold for multiple hypotheses testing was adjusted according to primarily testing the effect of hemodynamic response variability to the three Go/NoGo parameters of Correct Rejections, False alarms, and Hits, respectively, on level of IIVRT in ADHD (p<0.017; Bonferroni 0.05/3). For the bootstrapping procedure, p <.05 was used. In all the stepwise regression models, the variance inflation factor (VIF) was < 2.

Results

fMRI data independent component (IC) maps

The ICA resulted in 32 Go/NoGo task-correlated ICs, 8 of which represented regions in the DMN (see Figure 1 and Supplemented Table 1). IC 35, IC 39, IC44, IC 53, IC 71, and IC 74 showed posterior DMNs. IC 35 and IC 44 showed an intensity peak in the PCC, whereas IC 71 and IC 74 represent dorsal and ventral precuneus, respectively. IC 39 and 53 correlated highly with the posterior DMN regions as well. However, the posterior DMN in IC 53 correlated also with the superior parietal lobule on the lateral surface that is contiguous with precuneus, and in IC 39, the PCC correlated with mid-cingulate regions that is not typically recognized as a DMN region. IC 50 and IC 70 represented anterior DMNs with intensity peaks in the vmPFC, and IC 70 showed an extended involvement of the PCC. The other ICs represented among others a bilateral superior temporal network (IC 15), a right post-motor system network (IC 18) and attention-related networks (see Supplemental Table 1).

Preliminary descriptive analyses

The group of adolescents with ADHD and healthy controls matched in age and sex distributions, whereas the adolescents with ADHD had lower IQ than the healthy controls (see Table 1). ADHD-diagnosed adolescents had higher IIVRT compared with the healthy controls,

after conducting ANCOVAs controlling for effects of age, sex, full-scale IQ, and mean reaction times. Mean reaction time did not differ between study groups. In the ANCOVAs, age ($F(1,104)=8.25$, $p=0.005$) and mean reaction times ($F(1,104)=10.01$, $p=0.002$) covaried with level of IIVRT, whereas sex and full-scale IQ did not. Bivariate correlations showed that lower age correlated with higher IIVRT, females showed a higher IIVRT than males, and higher IIVRT correlated with higher mean reaction times (see Supplementary Table 2).

Variability in hemodynamic responses on level of IIVRT

Correct Rejections. The bootstrapped regression model that predicted maximized variance of IIVRT included a significant interaction effect between higher variability in hemodynamic responses to Correct Rejections in a bilateral, posterior DMN (IC 44) and ADHD. Higher amplitude variability in IC 44 specifically in ADHD predicted higher IIVRT (see Figure 1 and Table 2). In addition, the regression model included significant main effects of higher variability in hemodynamic responses to correct rejections in a bilateral posterior DMN (IC 74) and a right post-motor system to predict lower IIVRT (IC 18 (see Table 2). ADHD diagnosis and lower age predicted higher IIVRT, whereas sex or IQ did not. Bivariate correlation analyses showed that hemodynamic response variability to Correct Rejections in IC 44 correlated positively with hemodynamic response variability to Correct Rejections in IC 74; however, not with hemodynamic response variability to Correct Rejections in IC 18 or with level of IIVRT, mean reaction times, age, sex, or full-scale IQ (see Supplementary Table 3). Variability in hemodynamic responses to Correct Rejections in IC 74 correlated negatively with level of IIVRT and not with hemodynamic response variability to Correct Rejections in IC 18, mean reaction times, age, sex, or full-scale IQ.

False Alarms and Hits. The results from the stepwise regression analyses of hemodynamic response variability to False Alarms and Hits as predictors, respectively, showed that only a diagnosis of ADHD and the covariate of lower age significantly predicted higher IIVRT, and not variability in hemodynamic responses, sex, or full-scale IQ (see right-hand columns of Table 2, Supplementary Table 4, and Supplementary Table 5).

Mean amplitude of hemodynamic responses on level of IIVRT

Correct Rejections. The results from the bootstrapped regression model that predicted maximized variance showed no significant effects of mean hemodynamic responses on level of IIVRT. A diagnosis of ADHD and lower age did significantly predict higher IIVRT, whereas sex and full-scale IQ did not.

False Alarms. The model generated from the stepwise regression analysis showed that a significant interaction effect between amplitude mean to False Alarms in a bilateral superior temporal cortex with extensions to insula (IC 15) and a diagnosis of ADHD predicted higher IIVRT. Higher amplitude variability in IC 15 specifically predicted higher IIVRT in ADHD. In addition, a diagnosis of ADHD and lower age predicted higher IIVRT as main effects, whereas sex and IQ did not.

Hits. The results from the bootstrapped regression model that predicted maximized variance showed significant interaction effects between amplitude means to Hits in IC 37 and IC 62, respectively, and ADHD on IIVRT. In addition, main effects appeared of mean amplitude in IC 18 and a diagnosis of ADHD, respectively, to predict higher IIVRT together with a lower age. Sex and IQ did not predict level of IIVRT.

Discussion

The aim of the current study was to learn how functional brain network response variability or its strength of task engagement would predict attentional lapses, i.e., high IIVRT, in ADHD. As predicted, we found posterior DMN region variability in hemodynamic responses (IC 44 and IC 74), but not means, predicted level of IIVRT measured by behavioral performance on the Go/NoGo task. Higher variability in a PCC DMN (IC 44) predicted higher IIVRT only in ADHD. In contrast, variability in brain response for a precuneus DMN (IC 74) predicted lower IIVRT both in ADHD and healthy controls. Further, mean amplitude of hemodynamic responses in a bilateral superior temporal network with extensions to insula (IC 15) specifically predicted higher IIVRT in ADHD and not healthy controls. These findings appear to be the first that show posterior DMN is involved in fluctuation of attention in ADHD. This can be viewed as an important confirmation of the DMN hypothesis (16) since the posterior DMN node was originally showed to have the highest spontaneous fluctuations during resting state (13, 26). We did, however, not find as expected an effect of moment-to-moment fluctuations in the anterior DMN regions or an ADHD-specific effect of mean hemodynamic responses in right motor systems on level of attentional lapses. The results can be viewed as an additional support for the DMN hypothesis (16) since the posterior DMN node was originally showed to have the highest spontaneous fluctuations during resting state (13, 26). But importantly, the findings provide another clear indication that the consistency with which specific brain regions – especially the DMN – engage from trial-to-trial are particularly important to understanding the neurobiology of attentional lapses in ADHD.

Variability of hemodynamic responses elicited by correctly rejected NoGo stimuli played different roles in ADHD for different posterior DMN brain regions. For the PCC (IC 44), greater inconsistency of activation predicted higher IIVRT for ADHD adolescents, but the precuneus (IC

74) more inconsistent responses led to lower IIVRT. In many fMRI studies, the PCC and precuneus comprise one DMN subnetwork, and the specific role of each of these DM-subnetworks are not studied in accordance with recommendations from a recent study (54). The precuneus is recognized to be a functional core hub in connection with other functional networks that has an important role monitoring and regulating attention fluctuations(25), possibly rapidly adjusting attention resources in response to contextual changes. The schism in ADHD between brain variability versus behavioral variability for these two regions that normally closely co-engage across different task contexts emphasizes their dysfunction in ADHD. Thus, higher variability in hemodynamic responses in ADHD may not only be a potential marker of poorer attention functioning, but might provide a clue that important intra-network dysfunction or disconnection might be a specific factor that gives rise to abnormal IIVRT. This underscores the importance of studying study-elicited brain function; resting-state fMRI studies can only show high/low DMN activity fluctuations compared to control groups, whereas task-based studies can additionally quantify the consistency of that activity in different task-relevant contexts.

Interestingly, similar to previous fMRI studies using go/NoGo tasks (30-32), there was no evidence in this study that anterior DMN areas were involved in IIVRT. In contrast, such evidence has been found in other fMRI studies, but it is not currently clear if the task choice (e.g., oddball (23, 24) versus working memory (22)) or the fact that some of those tasks were self-paced might be responsible for anterior DMN involvement in IIVRT. But overall, the simple difference in IIVRT-related findings confirms that the consistency of anterior and posterior DMN areas will depend on task characteristics (55). We speculate that speeded reaction time tasks requiring a higher load on sustained attention compared to self-paced tasks might involve posterior DMN due to requirements of sustaining voluntary-controlled neural brain activation over time. Regardless of what future experimentation might show to be the explanation, this is a

clear call to continue to examine the neural correlates of IIVRT using a variety of different paradigms for a more complete understanding.

We also found specifically for adolescents with ADHD that higher IIVRT was predicted by mean hemodynamic responses to failed NoGo responses (false alarms) in a bilateral superior temporal network with extensions medially to insula (IC 15). To our knowledge, three prior studies linked the average levels of hemodynamic responses in temporal lobes to how much IIVRT is observed in ADHD (23, 32, 56). In one of these studies (23), including a small sample of boys with ADHD, higher mean hemodynamic responses in a superior temporal cortex network with extensions to insula associated with lower IIVRT on a visual oddball task similarly as in our study only among the healthy controls. The superior temporal lobes are mostly known for the involvement in language processing and as the location of the primary auditory cortex. However, several studies have shown that this brain area also is important to attention allocation (57). Interestingly, the Rubia et al. (23) study showed that lower mean hemodynamic responses bilaterally in superior and medial temporal cortices to a visual oddball stimuli that requires attention orientation (58) appeared only in the ADHD group. Studies including non-ADHD samples have shown brain activation in the superior temporal lobes being involved in involuntary orienting attention (58). Further, the insula, part of IC 15, is a critical node in the salience network involved in alerting/arousal attention, which typically interacts with involuntary orienting attention (59). Collectively, these observations raise the possibility the adolescents with ADHD in our study might have been distracted by external/internal salient stimuli when they were to focus on inhibiting motor responses. Alternatively, this IIVRT-temporal lobe relationship might reflect brain activity related to some sort of compensatory mechanism to help direct attention, secondary to the posterior DMN abnormalities we observed in the ADHD group.

Both higher mean and variability of hemodynamic responses across the Go/NoGo parameters in a right hemisphere postcentral gyrus motor system (IC 18) predicted higher IIVRT both in the adolescents with ADHD and healthy controls. Further, mean amplitudes to hits in IC 37 and IC 62, respectively, predicted higher IIVRT specifically in ADHD and not healthy controls. Important to note is that the Go/NoGo task used in the current study included a jittering design by varying inter-stimulus-intervals. The jittering design can introduce challenges in reliably isolating hemodynamic response amplitude or variability to the Go responses (Hits) across trials (60). Compounding this, the 'X' stimuli were frequent and rapid enough to nearly saturate the hemodynamic response to this condition. As such, Hit-related findings should perhaps be interpreted conservatively until they have been replicated.

Study strengths included the aim to address the inconsistent results of prior fMRI IIVT ADHD studies by using a moderate-sized samples to lend confidence in the results, by employing a data-reduction ICA methodology to concurrently consider all major brain network regions in the same analysis in a statistically efficient way, and by using data-driven hypothesis-testing to remain unconstrained by rigid theoretical assumptions of the neurobiological underpinnings of high IIVRT in ADHD. In contrast, while the current sample arguably provided higher power in the statistical analyses than typical fMRI studies of ADHD, our findings can be due to specific sample characteristics and needs to be replicated in larger studies.

Conclusion

Higher IIVRT has in general been recognized as a marker of poorer brain health (61) and to predict all-cause mortality in adults (62). Further, moment-to-moment fluctuations of brain signaling also has been suggested as an important parameter of brain health (36, 52). This not only emphasizes the general importance of better understanding the neural mechanisms that give

rise to IIVRT, it underscores the need to characterize how dysfunction in this neurobiology yields the typically high IIVRT found in most patients with ADHD. Such a mechanistic understanding could be quite important, as there already is evidence that higher amplitude variability in resting-state fMRI (Nomi et al., 2018) and during fMRI attention processing (56) predict higher ADHD symptom severity. As such, IIVRT-related neural dysfunction in ADHD holds potential to be treatment target for the disorder. Our findings suggest that variability in hemodynamic responses in posterior DMN elicited on rapid tests with high cognitive demands are important correlates of higher IIVRT during Go/NoGo task performance for ADHD-diagnosed adolescents.

References

1. Polanczyk G, Jensen P (2008): Epidemiologic considerations in attention deficit hyperactivity disorder: a review and update. *Child Adolesc Psychiatr Clin N Am*. 17:245–260, vii.
2. Castellanos FX, Tannock R (2002): Neuroscience of attention–deficit/hyperactivity disorder: the search for endophenotypes. *Nature reviews Neuroscience*. 3:617–628.
3. Kofler MJ, Rapport MD, Sarver DE, Raiker JS, Orban SA, Friedman LM, et al. (2013): Reaction time variability in ADHD: a meta–analytic review of 319 studies. *Clin Psychol Rev*. 33:795–811.
4. Kuntsi J, Klein C (2012): Intraindividual variability in ADHD and its implications for research of causal links. *Current topics in behavioral neurosciences*. 9:67–91.
5. Tamm L, Narad ME, Antonini TN, OBrien KM, Hawk LW, Jr., Epstein JN (2012): Reaction time variability in ADHD: a review. *Neurotherapeutics : the journal of the American Society for Experimental NeuroTherapeutics*. 9:500–508.
6. Weissman DH, Roberts KC, Visscher KM, Woldorff MG (2006): The neural bases of momentary lapses in attention. *Nature neuroscience*. 9:971–978.
7. Epstein JN, Langberg JM, Rosen PJ, Graham A, Narad ME, Antonini TN, et al. (2011): Evidence for higher reaction time variability for children with ADHD on a range of cognitive tasks including reward and event rate manipulations. *Neuropsychology*. 25:427–441.
8. Karalunas SL, Geurts HM, Konrad K, Bender S, Nigg JT (2014): Annual research review: Reaction time variability in ADHD and autism spectrum disorders: measurement and mechanisms of a proposed trans–diagnostic phenotype. *Journal of child psychology and psychiatry, and allied disciplines*. 55:685–710.
9. Bellgrove MA, Hawi Z, Kirley A, Gill M, Robertson IH (2005): Dissecting the attention deficit hyperactivity disorder (ADHD) phenotype: sustained attention, response variability and spatial attentional asymmetries in relation to dopamine transporter (DAT1) genotype. *Neuropsychologia*. 43:1847–1857.
10. Kuntsi J, Oosterlaan J, Stevenson J (2001): Psychological mechanisms in hyperactivity: I. Response inhibition deficit, working memory impairment, delay aversion, or something else? *Journal of child psychology and psychiatry, and allied disciplines*. 42:199–210.
11. Antonini TN, Narad ME, Langberg JM, Epstein JN (2013): Behavioral correlates of reaction time variability in children with and without ADHD. *Neuropsychology*. 27:201–209.

12. Adamo N, Hodsoll J, Asherson P, Buitelaar JK, Kuntsi J (2019): Ex–Gaussian, Frequency and Reward Analyses Reveal Specificity of Reaction Time Fluctuations to ADHD and Not Autism Traits. *J Abnorm Child Psychol*. 47:557–567.
13. Raichle ME, MacLeod AM, Snyder AZ, Powers WJ, Gusnard DA, Shulman GL (2001): A default mode of brain function. *Proceedings of the National Academy of Sciences of the United States of America*. 98:676–682.
14. Shulman GL, Fiez JA, Corbetta M, Buckner RL, Miezin FM, Raichle ME, et al. (1997): Common Blood Flow Changes across Visual Tasks: II. Decreases in Cerebral Cortex. *J Cogn Neurosci*. 9:648–663.
15. Castellanos FX, Kelly C, Milham MP (2009): The restless brain: attention–deficit hyperactivity disorder, resting–state functional connectivity, and intrasubject variability. *Can J Psychiatry*. 54:665–672.
16. Sonuga–Barke EJ, Castellanos FX (2007): Spontaneous attentional fluctuations in impaired states and pathological conditions: a neurobiological hypothesis. *Neuroscience and biobehavioral reviews*. 31:977–986.
17. Castellanos FX, Margulies DS, Kelly C, Uddin LQ, Ghaffari M, Kirsch A, et al. (2008): Cingulate–precuneus interactions: a new locus of dysfunction in adult attention–deficit/hyperactivity disorder. *Biological psychiatry*. 63:332–337.
18. Choi J, Jeong B, Lee SW, Go HJ (2013): Aberrant development of functional connectivity among resting state–related functional networks in medication–naive ADHD children. *PLoS One*. 8:e83516.
19. Fair DA, Posner J, Nagel BJ, Bathula D, Dias TG, Mills KL, et al. (2010): Atypical default network connectivity in youth with attention–deficit/hyperactivity disorder. *Biological psychiatry*. 68:1084–1091.
20. Sripada C, Kessler D, Fang Y, Welsh RC, Prem Kumar K, Angstadt M (2014): Disrupted network architecture of the resting brain in attention–deficit/hyperactivity disorder. *Hum Brain Mapp*. 35:4693–4705.
21. Sun L, Cao Q, Long X, Sui M, Cao X, Zhu C, et al. (2012): Abnormal functional connectivity between the anterior cingulate and the default mode network in drug–naive boys with attention deficit hyperactivity disorder. *Psychiatry Res*. 201:120–127.
22. Fassbender C, Zhang H, Buzy WM, Cortes CR, Mizuiri D, Beckett L, et al. (2009): A lack of default network suppression is linked to increased distractibility in ADHD. *Brain research*. 1273:114–128.
23. Rubia K, Smith AB, Brammer MJ, Taylor E (2007): Temporal lobe dysfunction in medication–naive boys with attention–deficit/hyperactivity disorder during attention allocation and its relation to response variability. *Biological psychiatry*. 62:999–1006.

24. Sørensen L, Eichele T, van Wageningen H, Plessen KJ, Stevens MC (2016): Amplitude variability over trials in hemodynamic responses in adolescents with ADHD: The role of the anterior default mode network and the non-specific role of the striatum. *Neuroimage Clin*. 12:397-404.
25. Cavanna AE, Trimble MR (2006): The precuneus: a review of its functional anatomy and behavioural correlates. *Brain*. 129:564-583.
26. Greicius MD, Krasnow B, Reiss AL, Menon V (2003): Functional connectivity in the resting brain: a network analysis of the default mode hypothesis. *Proceedings of the National Academy of Sciences of the United States of America*. 100:253-258.
27. Cortese S, Kelly C, Chabernaud C, Proal E, Di Martino A, Milham MP, et al. (2012): Toward systems neuroscience of ADHD: a meta-analysis of 55 fMRI studies. *Am J Psychiatry*. 169:1038-1055.
28. Hart H, Radua J, Nakao T, Mataix-Cols D, Rubia K (2013): Meta-analysis of functional magnetic resonance imaging studies of inhibition and attention in attention-deficit/hyperactivity disorder: exploring task-specific, stimulant medication, and age effects. *JAMA Psychiatry*. 70:185-198.
29. Lei D, Du M, Wu M, Chen T, Huang X, Du X, et al. (2015): Functional MRI reveals different response inhibition between adults and children with ADHD. *Neuropsychology*. 29:874-881.
30. Siniatchkin M, Glatthaar N, von Muller GG, Prehn-Kristensen A, Wolff S, Knochel S, et al. (2012): Behavioural treatment increases activity in the cognitive neuronal networks in children with attention deficit/hyperactivity disorder. *Brain Topogr*. 25:332-344.
31. Suskauer SJ, Simmonds DJ, Caffo BS, Denckla MB, Pekar JJ, Mostofsky SH (2008): fMRI of intrasubject variability in ADHD: anomalous premotor activity with prefrontal compensation. *Journal of the American Academy of Child and Adolescent Psychiatry*. 47:1141-1150.
32. Spinelli S, Vasa RA, Joel S, Nelson TE, Pekar JJ, Mostofsky SH (2011): Variability in post-error behavioral adjustment is associated with functional abnormalities in the temporal cortex in children with ADHD. *Journal of child psychology and psychiatry, and allied disciplines*. 52:808-816.
33. van Belle J, van Raalten T, Bos DJ, Zandbelt BB, Oranje B, Durston S (2015): Capturing the dynamics of response variability in the brain in ADHD. *Neuroimage Clin*. 7:132-141.
34. Mostofsky SH, Simmonds DJ (2008): Response inhibition and response selection: two sides of the same coin. *J Cogn Neurosci*. 20:751-761.

35. Stevens MC, Pearlson GD, Calhoun VD, Bessette KL (2018): Functional Neuroimaging Evidence for Distinct Neurobiological Pathways in Attention–Deficit/Hyperactivity Disorder. *Biol Psychiatry Cogn Neurosci Neuroimaging*. 3:675–685.
36. Boylan MA, Foster CM, Pongpipat EE, Webb CE, Rodrigue KM, Kennedy KM (2021): Greater BOLD Variability is Associated With Poorer Cognitive Function in an Adult Lifespan Sample. *Cereb Cortex*. 31:562–574.
37. Eichele T, Debener S, Calhoun VD, Specht K, Engel AK, Hugdahl K, et al. (2008): Prediction of human errors by maladaptive changes in event–related brain networks. *Proceedings of the National Academy of Sciences of the United States of America*. 105:6173–6178.
38. Suskauer SJ, Simmonds DJ, Fotedar S, Blankner JG, Pekar JJ, Denckla MB, et al. (2008): Functional magnetic resonance imaging evidence for abnormalities in response selection in attention deficit hyperactivity disorder: differences in activation associated with response inhibition but not habitual motor response. *J Cogn Neurosci*. 20:478–493.
39. Kaufman J, Birmaher B, Brent D, Rao U, Flynn C, Moreci P, et al. (1997): Schedule for Affective Disorders and Schizophrenia for School–Age Children–Present and Lifetime Version (K–SADS–PL): initial reliability and validity data. *Journal of the American Academy of Child and Adolescent Psychiatry*. 36:980–988.
40. Kadesjo B, Gillberg C (2001): The comorbidity of ADHD in the general population of Swedish school–age children. *Journal of child psychology and psychiatry, and allied disciplines*. 42:487–492.
41. Wechsler D (1999): *Wechsler Abbrievated Scale of Intelligence. WASI. Manual.* San Antonio, Tex: The Psychological Corporation.
42. Stevens MC, Kiehl KA, Pearlson GD, Calhoun VD (2007): Functional neural networks underlying response inhibition in adolescents and adults. *Behav Brain Res*. 181:12–22.
43. Jenkinson M, Bannister P, Brady M, Smith S (2002): Improved optimization for the robust and accurate linear registration and motion correction of brain images. *Neuroimage*. 17:825–841.
44. Jenkinson M, Beckmann CF, Behrens TE, Woolrich MW, Smith SM (2012): Fsl. *Neuroimage*. 62:782–790.
45. Andersson JL, Hutton C, Ashburner J, Turner R, Friston K (2001): Modeling geometric deformations in EPI time series. *Neuroimage*. 13:903–919.
46. Cox RW (1996): AFNI: software for analysis and visualization of functional magnetic resonance neuroimages. *Comput Biomed Res*. 29:162–173.

47. Griffanti L, Salimi–Khorshidi G, Beckmann CF, Auerbach EJ, Douaud G, Sexton CE, et al. (2014): ICA–based artefact removal and accelerated fMRI acquisition for improved resting state network imaging. *Neuroimage*. 95:232–247.
48. Abou–Elseoud A, Starck T, Remes J, Nikkinen J, Tervonen O, Kiviniemi V (2010): The effect of model order selection in group PICA. *Human brain mapping*. 31:1207–1216.
49. Kiviniemi V, Starck T, Remes J, Long X, Nikkinen J, Haapea M, et al. (2009): Functional segmentation of the brain cortex using high model order group PICA. *Human brain mapping*. 30:3865–3886.
50. Bell AJ, Sejnowski TJ (1995): An information–maximization approach to blind separation and blind deconvolution. *Neural computation*. 7:1129–1159.
51. Erhardt EB, Rachakonda S, Bedrick EJ, Allen EA, Adali T, Calhoun VD (2011): Comparison of multi–subject ICA methods for analysis of fMRI data. *Human brain mapping*. 32:2075–2095.
52. Mohr PN, Nagel IE (2010): Variability in brain activity as an individual difference measure in neuroscience? *J Neurosci*. 30:7755–7757.
53. Leys C, Lay C, Klein O, Bernard P, Licata L (2013): Detecting outliers: do not use standard deviation around the mean, use absolute deviation aroudn the median. *Journal of Experimental Social Psychology*. 49:764–766.
54. Wang S, Tepfer LJ, Taren AA, Smith DV (2020): Functional parcellation of the default mode network: a large–scale meta–analysis. *Sci Rep*. 10:16096.
55. Andrews–Hanna JR, Smallwood J, Spreng RN (2014): The default network and self–generated thought: component processes, dynamic control, and clinical relevance. *Annals of the New York Academy of Sciences*. 1316:29–52.
56. Depue BE, Burgess GC, Willcutt EG, Bidwell LC, Ruzic L, Banich MT (2010): Symptom–correlated brain regions in young adults with combined–type ADHD: their organization, variability, and relation to behavioral performance. *Psychiatry Res*. 182:96–102.
57. Kobel M, Bechtel N, Specht K, Klarhofer M, Weber P, Scheffler K, et al. (2010): Structural and functional imaging approaches in attention deficit/hyperactivity disorder: does the temporal lobe play a key role? *Psychiatry Res*. 183:230–236.
58. Kim H (2014): Involvement of the dorsal and ventral attention networks in oddball stimulus processing: a meta–analysis. *Hum Brain Mapp*. 35:2265–2284.
59. Posner MI (2012): Attentional networks and consciousness. *Front Psychol*. 3:64.
60. Amaro E, Jr., Barker GJ (2006): Study design in fMRI: basic principles. *Brain Cogn*. 60:220–232.

61. MacDonald SW, Nyberg L, Backman L (2006): Intra–individual variability in behavior: links to brain structure, neurotransmission and neuronal activity. *Trends Neurosci*. 29:474–480.
62. Shipley BA, Der G, Taylor MD, Deary IJ (2006): Cognition and all–cause mortality across the entire adult age range: health and lifestyle survey. *Psychosom Med*. 68:17–24.

Table 1. Descriptive information about the groups of adolescents with ADHD and healthy controls.

	ADHD			HC		Analysis		
Variables	Mean	SD		Mean	SD	*t*	*f*#	*f*##
Age	15.297	1.80		15.476	1.75	-0.53		
Full-Scale IQ	105.345	13.4649		110.628	10.0780	-2.329*		
Mean RT	0.3776	0.04069		0.3716	0.03929	0.79	0.31	
IIVRT	0.1416	0.04917		0.1058	0.03298	4.480**	17.80**	17.79**
	n males	*n* females		*n* males	*n* females			
Sex	43	12		43	12			

Note. **$p < .001$; *$p < .05$. RT = reaction times; IIVRT = intra-individual variability in reaction times; #= between-group effects adjusted for distribution of age, sex, and Full-scale IQ (df = 1,105); ##= between-group effect adjusted for distribution of Mean RT, age, sex, and Full-scale IQ (df = 1,104).

Table 2. Maximized predicted variance from stepwise linear regression analyses of hemodynamic responses on ADHD IIVRT - the last model with highest explained variance with p<.017 selected.

Hemodynamic response variability to go/no-go correct rejections (CR):								Bootstrapping:			
Predictors	*Adj. R^2*	*df*	*F*	*p*	B	*β*	*p*	*p*	SE	95% CI for B	
Age	0.38	101	9.20	<0.001	-0.007	-0.29	<0.001*	0.002	0.002	-0.010	-0.003
Sex					-0.004	-0.04	0.631	0.657	0.009	-0.024	0.012
Full-scale IQ					0.000	-0.08	0.287	0.324	0.000	-0.001	0.000
ADHD					0.030	0.33	<0.001*	0.001	0.007	0.015	0.044
CR_IC18_SD					-0.003	-0.22	0.006*	0.005	0.001	-0.005	-0.001
CR_IC74_SD					-0.005	-0.23	0.004*	0.005	0.002	-0.009	-0.002
ADHD*CR_IC15_SD					0.015	0.21	0.01	0.055	0.008	-0.001	0.030
ADHD*CR_IC44_SD					0.017	0.20	0.014*	0.029	0.008	0.000	0.030
Hemodynamic response mean to go/no-go false alarms (FA):								Bootstrapping:			
Predictors	*Adj. R^2*	*df*	*F*	*p*	B	*β*	*p*	*p*	SE	*p* 95% CI	
Age	0.28	104	9.66	<.001	-0.006	-0.23	0.008*	0.002	0.002	-0.009	-0.002
Sex					-0.012	-0.11	0.199	0.252	0.010	-0.031	0.008
WASI Full-scale IQ					0.000	-0.08	0.359	0.422	0.000	-0.001	0.000
ADHD					0.034	0.27	<0.001*	0.001	0.008	0.018	0.048
ADHD*CR_IC15_M					0.018	0.28	0.001*	0.005	0.006	0.006	0.031
Hemodynamic response mean to go/no-go hits:								Bootstrapping:			
Predictors	*djsuted R*	*df*	*F*	*p*	B	*β*	*p*	*p*	SE	*p* 95% CI	
Age	0.37	102	10.25	<.001	-0.008	-0.30	<0.001*	0.001	0.002	-0.011	-0.004
Sex					-0.004	-0.03	0.67	0.690	0.010	-0.023	0.014
WASI Full-scale IQ					1.232E-5	0.00	0.97	0.969	0.000	-0.001	0.001
ADHD					0.034	0.38	<0.001*	0.001	0.007	0.019	0.048
Hits_IC18_M					-0.029	-0.28	<0.001*	0.001	0.006	-0.040	-0.017
ADHD*Hits_IC37_M					-0.019	-0.21	0.008*	0.014	0.010	-0.042	0.001
ADHD*Hits_IC62_M					-0.013	-0.21	0.01*	0.027	0.006	-0.024	0.001
Models^ with no predictions of hemodynamic responses on IIVRT:								Bootstrapping:			
Predictors	*Adj. R^2*	*df*	*F*	*p*	B	*β*	*p*	*p*	SE	95% CI for B	
Age	0.21	105	8.29	.001	-0.007	-0.26	0.003*	0.005*	0.002	-0.011	-0.003
Sex					-0.007	-0.07	0.455	0.500	0.010	-0.029	0.012
WASI Full-scale IQ					0.000	-0.07	0.462	0.507	0.000	-0.001	0.001
ADHD					0.033	0.37	<0.001*	0.001*	0.008	0.017	0.050

Note. *p <0.017 + p <0.05 in the bootstrapped resampling procedure; #= bootstrapped regression models; ^= regression models with no ICs predicting IIVRT = hemodynamic response variability to false alarms (FA) or hits, and further, hemodynamic response mean to correct rejections (CR); Adj. = adjusted; SE = standard error.

a) Amplitude Variability to Correct Rejections:

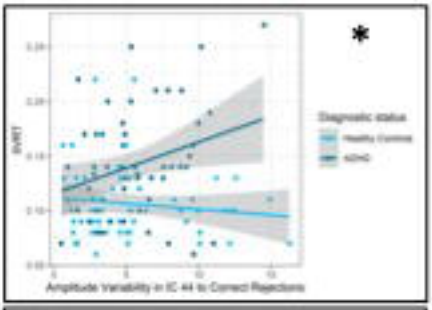

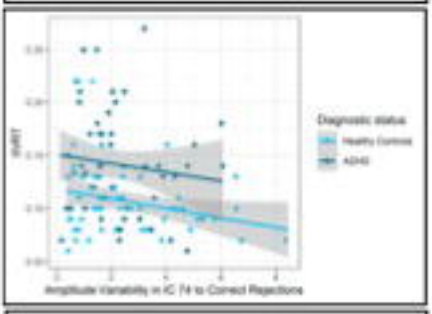

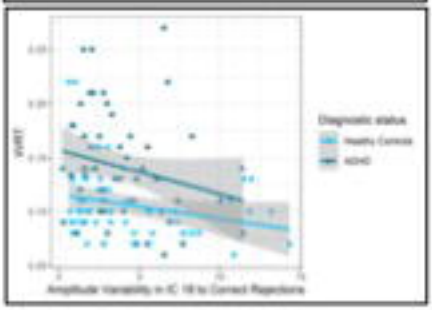

b) Amplitude Mean to False Alarms:

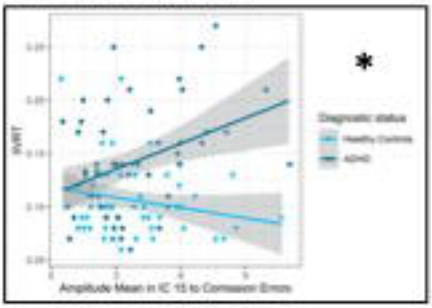

c) Brain Networks:

IC 44 Bilateral Posterior Cingulate (DMN)

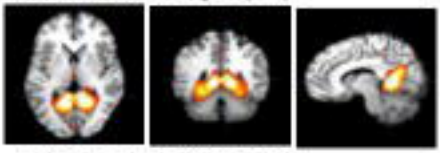

Max Peak: X = 8 Y = -44 Z = 6; t = 19.46

IC 74 Bilateral Precuneus (DMN)

Max Peak: X = 14 Y = -66 Z = 26; t = 15.74

IC 18 Right Postcentral Gyrus

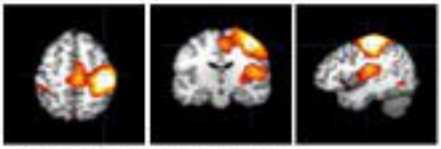

Max Peak: X = 44 Y = -24 Z = 52; t = 21.88

IC 15 Bilateral Superior Temporal Cortex

Max Peak: X = 66 Y = -11 Z = 8 ; t = 25.72

* Interaction Effect between IC and ADHD